Modified picket fence porphyrin Fe(III) and Zn(II) complexes as a model for hemoglobin mutants

Hiroyasu Imai*, Shigeo Nakagawa and Eishin Kyuno*

Department of Pharmaceutical Science, School of Pharmacy, Hokuriku University, 3 Ho Kanagawa-Machi, Kanazawa 920-11 (Japan)

(Received September 23, 1991)

Abstract

Zinc(II) and iron(III) complexes of three modified picket fence porphyrins in which one of the four pivalamido pickets was replaced by a *meta*-methyl, -amino, or -hydroxy benzoylamino picket were synthesized. The iron complex containing the phenolic OH on the picket fence mimics the abnormal active sites for a type of hemoglobin mutant, Hb M. Proton NMR and visible spectra for the zinc complexes have shown that the NH_2 or OH group on the picket fence does not coordinate to the central metal ion in CH_2Cl_2 at room temperature. Contrary to this, coordination of the phenolic OH (or O^-) on the picket fence to form O–Fe–O axial geometry was found for the iron complex by ESR measurements in CH_2Cl_2 at 77 K. On the other hand, the ESR spectra for the three iron complexes with 1-methylimidazole under basic conditions have shown the presence of two regioisomers in O–Fe–N axial geometry, because of the unsymmetrical distribution of the picket fences on the porphyrin plane.

Introduction

A type of hemoglobin mutant, Hb M, is different from normal hemoglobin (Hb A) in terms of containing tyrosines instead of distal or proximal histidines in either the α or β chain [1]. These are comprised of Hb M Boston ($\alpha^{58\ His\rightarrow Tyr}$) [2], Hb M Iwate ($\alpha^{87\ His\rightarrow Tyr}$) [3], Hb M Saskatoon ($\beta^{63\ His\rightarrow Tyr}$) [4], and Hb M Hyde Park ($\beta^{92\ His\rightarrow Tyr}$) [3b]. The iron atoms in the abnormal chains are permanently oxidized to Fe(III) to which phenolic-O^- of the tyrosines is coordinated. Thereby, the remaining normal chains in these Hb M show abnormal behavior in O_2 affinity, Bohr effect and heme–heme interactions. However, the peculiar structure–function relationships revealed by the Hb M are not clear in detail.

A well-established approach to understand various structure–function relationships is to study proper models that are artificially synthesized, and a few works have been reported on models for abnormal hemoglobins. Ainscough *et al.* [5] have studied phenoxides of an Fe(III) porphyrin as a model for Hb M. Schaeffer *et al.* [6] have reported intramolecular coordination of alcoholic O^- to Fe(III) ion in a 'basket-handle' porphyrin complex in a basic condition. On the other hand, one of the most successful models for Hb is picket fence porphyrin complexes developed by Collman *et al.* [7, 8]. In this work we have attempted to incorporate a phenol group into the picket fence porphyrin as shown in Fig. 1, and to make comparisons of its metal complexes

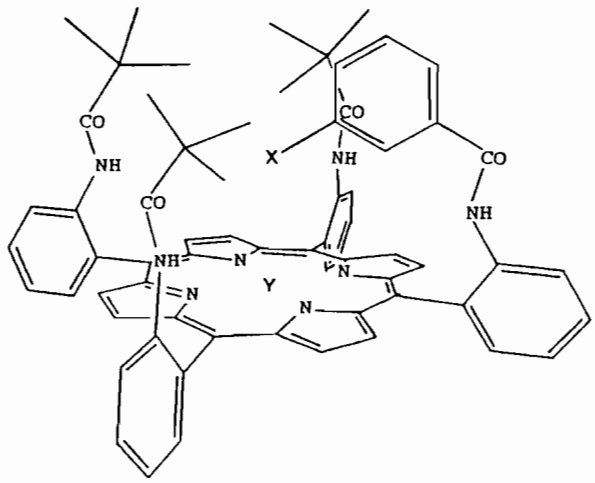

X	Y		
	2H	Zn(II)	Fe(III)Br
CH_3	1a	1b	1c
NH_2	2a	2b	2c
OH	3a	3b	3c

Fig. 1. Modified 'picket fence' porphyrins.

*Authors to whom correspondence should be addressed.

0020-1693/92/$5.00

with the related complexes of a porphyrin that contains $-CH_3$ or $-NH_2$ instead of -OH on the phenolic picket.

Experimental

Measurements

Proton NMR spectra were measured on a JEOL FX-100 spectrometer. ESR spectra at X band were obtained from a JEOL JES-FE2GX spectrometer. Visible absorption spectra were recorded on a Hitachi 340 spectrophotometer. The equilibrium constants for zinc complexes with pyridine were determined from the Hill equation on the basis of spectrophotometric titrations of pyridine as described elsewhere [9].

Materials

Nitrogenous bases, pyridine (py), 1-methylimidazole (1-MeIm) and tributylamine (TBA) were purified by vacuum distillation. Toluene and dichloromethane were distilled from molecular sieves (4A).

Syntheses

meso-5α,10α,15α-Tris(2-pivalamidophenyl)-20α-[2-(3-methylbenzoylamino)phenyl]porphyrin, H_2tPMBP (1a)

meso-5α,10α,15α-Tris(2-pivalamidophenyl)-20α-(2-aminophenyl)porphyrin, H_2tPamP was obtained by the published method [10]. To a solution of H_2tPamP in benzene (0.60 g/100 ml) containing *N*-methylmorpholine (2 ml), 3-methylbenzoyl chloride (3 ml) was added dropwise and then stirred for 5 h at room temperature. After drying on a rotary evaporator, the mixture was purified by silica-gel column chromatography (3×55 cm, $CHCl_3/(C_2H_5)_2O = 15/1$), yield 0.55 g (79%). *Anal.* Calc. for $C_{67}H_{64}N_8O_4$: C, 76.99; H, 6.17; N, 10.72. Found: C, 76.63; H, 6.07; N, 10.48%. ^{1}H NMR ($CDCl_3$): δ −2.56 (s, 2H) D_2O exchangeable, −0.01 (s, 18H), 0.10 (s, 9H), 1.45 (s, 3H), 5.89–6.01 (m, 2H), 6.54–6.62 (m, 2H), 7.22–8.01 (m, 16H), 8.72 (d, 4H), 8.85 (br.s, 8H).

meso-5α,10α,15α-Tris(2-pivalamidophenyl)-20α-[2-(3-aminobenzoylamino)phenyl]porphyrin H_2tPABP (2a)

meso-5α,10α,15α-Tris(2-pivalamidophenyl)-20α-[2-(3-nitrobenzoylamino)phenyl]porphyrin, H_2tPNBP, was prepared similarly to the case for H_2tPMBP using 3-nitrobenzoyl chloride instead of 3-methylbenzoyl chloride. To a solution of H_2tPNBP (0.62 g) in 70 ml of AcOH containing 6 ml of 6 N HCl, excess $SnCl_2 \cdot 2H_2O$ (6 g) was added and stirred for 4 h at room temperature. The mixture was cautiously neutralized with concentrated aqueous ammonia in an ice bath. Chloroform (100 ml) was added to the suspension and the mixture was stirred for 5 min. The $CHCl_3$ layer was separated and washed first with dilute aqueous ammonia then twice with water. The $CHCl_3$ solution was dried over anhydrous Na_2SO_4 then crystallized on an evaporator. The solid was purified by a silica-gel column (3×30 cm, $CHCl_3$), eluting with $CHCl_3/(CH_3)_2CO$ (20/1), yield 0.48 g (80%). *Anal.* Calc. for $C_{66}H_{63}N_9O_4 \cdot \frac{1}{2}CHCl_3$: C, 72.22; H, 5.79; N, 11.40. Found: C, 72.45; H, 6.02; N, 11.38%. ^{1}H NMR ($CDCl_3$): δ −2.57 (s, 2H) D_2O exchangeable, 0.02 (s, 18H), 0.10 (s, 9H), 3.15 (s, 2H) D_2O exchangeable, 5.04 (d, 1H), 5.67 (t, 1H), 6.02 (d, 1H), 6.44 (s, 1H), 7.19–7.95 (m, 16H), 8.70 (d, 4H), 8.82 (m, 8H).

meso-5α,10α,15α-Tris(2-pivalamidophenyl)-20α-[2-(3-hydroxybenzoylamino)phenyl]porphyrin, H_2tPHBP (3a)

meso-5α,10α,15α-Tris(2-pivalamidophenyl)-20α-[2-(3-acetoxybenzoylamino)phenyl]porphyrin, H_2tPATBP was prepared similarly to the case for H_2tPMBP using 3-acetoxybenzoyl chloride instead of 3-methylbenzoyl chloride. To a solution of H_2tPATBP (0.28 g) in 50 ml of acetone, 20 ml of 1 N NaOH was added. After stirring for 20 min at room temperature, oxalic acid solution (0.4 g/50 ml) was added to the mixture. The porphyrin was extracted with $CHCl_3$ (100 ml) from the mixture and was purified by a silica-gel column (3×25 cm, $CHCl_3/(C_2H_5)_2O = 5/1$, yield 0.25 g (93%). *Anal.* Calc. for $C_{66}H_{62}N_8O_5 \cdot CHCl_3$: C, 68.98; H, 5.44; N, 9.60. Found: C, 69.42; H, 5.45; N, 9.75%. ^{1}H NMR ($CDCl_3$): δ −2.76 (s, 2H) D_2O exchangeable, −0.06 (s, 18H), 0.14 (s, 9H), 4.88 (s, 1H), 6.15 (br.s, 1H), 6.42 (m, 2H), 7.22–8.12 (m, 16H), 8.64 (d, 4H), 8.89 (m, 8H).

Zinc(II) insertion

Porphyrins **1a–3a** were treated with $ZnCl_2$ according to the literature [9], yielding the corresponding Zn(II) complexes, **1b–3b**.

Zn(tPMBP) (1b)

Anal. Calc. for $C_{67}H_{62}N_8O_4Zn \cdot \frac{1}{3}CHCl_3$: C, 70.42; H, 5.47; N, 9.77. Found: C, 70.27; H, 5.47; N, 9.77%. ^{1}H NMR ($CDCl_3$): δ −0.19 (s, 18H), −0.08 (s, 9H), 1.47 (s, 3H), 5.52 (d, 1H), 5.86 (t, 1H), 6.5 (m, 2H), 7.11–7.93 (m, 16H), 8.50 (m, 4H), 8.83 (br.s, 8H). Vis (CH_2Cl_2): λ (nm) 419.6, 546.2, 583(sh).

Zn(tPABP) (2b)

Anal. Calc. for $C_{66}H_{61}N_9O_4Zn \cdot \frac{1}{2}CHCl_3$: C, 68.31; H, 5.30; N, 10.78. Found: C, 68.47; H, 5.20; N, 10.83. ^{1}H NMR ($CDCl_3$): δ −0.28 (s, 18H), −0.15 (s, 9H), 1.35 (br.s, 2H) D_2O exchangeable, 4.66 (d, 1H), 5.4 (m, 2H), 5.73 (s, 1H), 7.05 (s, 1H), 7.15 (s, 3H), 7.33–7.87 (m, 12H), 8.40 (m, 4H), 8.76 (s, 8H). Vis (CH_2Cl_2): λ (nm) 420.2, 546.6, 584(sh).

Zn(tPHBP) (3b)

Anal. Calc. for $C_{66}H_{60}N_8O_5Zn \cdot \frac{1}{3}CHCl_3$: C, 69.25; H, 5.29; N, 974. Found: C, 68.85; H, 5.26; N, 9.77%. ^1H NMR ($CDCl_3$): δ −0.28 (s, 18H), −0.10 (s, 9H), 5.44–6.51 (m, 5H), 7.26–7.80 (m, 16H), 8.23–8.45 (m, 4H), 8.74–8.78 (m, 8H). Vis (CH_2Cl_2): λ (nm) 420.8, 547.4, 584(sh).

Iron(III) insertion

Porphyrins **1a–3a** were treated with anhydrous $FeBr_2$ under N_2 atmosphere according to the literature [8], yielding the corresponding Fe(III) complexes, **1c–3c**.

Fe(tPMBP)Br (1c)

Anal. Calc. for $C_{67}H_{62}N_8O_4BrFe$: C, 68.25; H, 5.30; N, 9.50. Found: C, 68.59; H, 5.03; N, 9.45%. Vis (CH_2Cl_2): λ (nm) 417.0, 508.6, 580.8.

Fe(tPABP)Br (2c)

Anal. Calc. for $C_{66}H_{61}N_9O_4BrFe \cdot \frac{1}{3}CHCl_3$: C, 65.32; H, 5.07; N, 10.33. Found: C, 65.84; H, 5.17; N, 10.25%. Vis (CH_2Cl_2): λ (nm) 417.4, 509.8, 583.6.

Fe(tPHBP)Br (3c)

Anal. Calc. for $C_{66}H_{60}N_8O_5BrFe \cdot \frac{1}{2}CHCl_3$: C, 64.38; H, 4.92; N, 9.03. Found: C, 64.20; H, 4.89; N, 9.04%. Vis (CH_2Cl_2): λ (nm) 416.8, 511.4, 586.0.

Results and discussion

Relative position of pickets

Model building (CPK) has shown that the phenolic OH group of **3b** and **3c** is accessible to the critical distance capable of coordinating to the central metal ion, and that the position of the hydroxy group is restricted to move to some extent because of the rigidity of the phenyl picket. This organization of the hydroxy group suitably mimics the phenolic residue of tyrosine in Hb M. Further, ^1H NMR data for porphyrins have provided information on relative configurations among the pickets. The trimethyl signals of metal-free porphyrins, **1a–3a**, and their zinc complexes, **1b–3b**, are split with a ratio of 2:1; 18 protons of the methyl groups appear at higher field by 0.1–0.2 ppm than the other 9 protons. Since this phenomenon has not been observed for α^3,α'-type picket fence porphyrins containing no phenyl picket [10], these results can be understood in terms of ring-current shifts from the phenyl picket. The phenyl picket stands at the position between the adjacent two pivalamido pickets and the remaining pivalamido picket is nearly coplanar with the phenyl ring. Of course, the phenyl pickets of the porphyrins will not be so rigid but rotating as illustrated in Fig. 2, because the

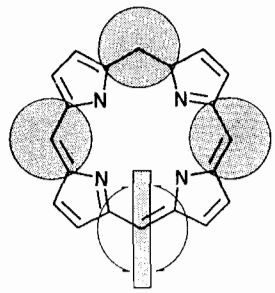

Fig. 2. Schematic representation of the orientation of the phenyl picket (rectangular box) relative to the pivalamido pickets (circles) in the prepared porphyrins.

methyl signal on the phenyl picket of **1a** (1.45 ppm) and that of **1b** (1.47 ppm) are not split.

Zinc complexes

As can be seen in 'Experimental', only slight differences are found in the visible spectral data of **1b, 2b** and **3b**. Contrary to this, the addition of aniline to **1b** in CH_2Cl_2 gave rise to a remarkable spectral change due to the coordination of $-NH_2$ of aniline to the zinc ion; Vis for Zn(tPMBP)($C_6H_5NH_2$): λ = 559, 598 nm. Thus, it is unlikely that, in the absence of nitrogenous bases, the NH_2 group in the phenyl picket of **2b** coordinates to the zinc ion. This is further supported by the fact that the binding constants of pyridine to **1b–3b** are very similar to each other; log K (25 °C in CH_2Cl_2) = 4.72, 4.72 and 4.52 for **1b, 2b** and **3b**, respectively. In the ^1H NMR spectra for the zinc complexes, **1b–3b**, the chemical shifts of the phenyl pickets lie between 4.7 and 6.5 ppm, and there are also little differences among these complexes. Additionally, these chemical shifts are found to be not so much changed from those of the corresponding metal-free porphyrins, **1a–3a**. If intramolecular coordination occured in **2b** or **3b**, the resonance signal of the 2-position of the phenyl pickets should be shifted to appreciably higher field, due to the increased π-current effect from the porphyrin plane. Therefore, these spectral data indicate that intra- or intermolecular coordination of NH_2 or OH in **2b** or **3b** cannot take place in these experimental conditions. This may be caused by a greater steric restriction on the position of the NH_2 or OH group than that expected from the model building stated earlier.

Iron complexes

In the case of iron complexes, the visible spectral data are also similar to each other, suggesting that ligation of NH_2 or OH of the phenyl picket in **3b** or **3c** does not occur. Figure 3 shows ESR spectra for low-spin Fe(III) species in CH_2Cl_2 at 77 K, and their g values are listed in Table 1. The relative intensities of the three types of spectra changed with the mole

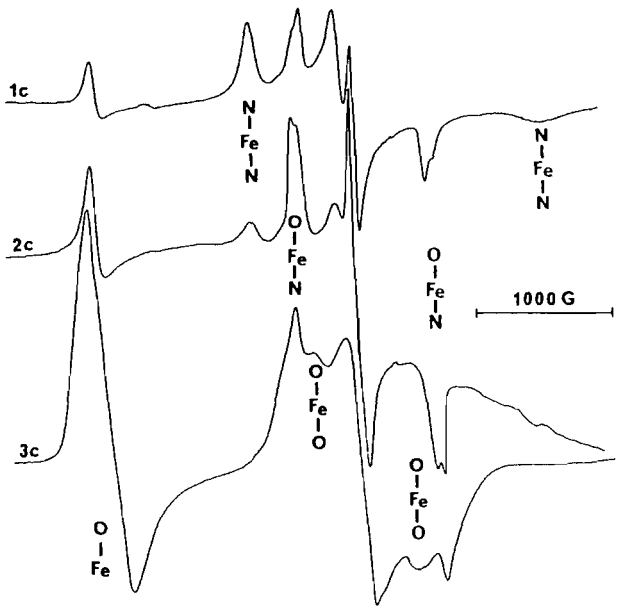

Fig. 3. ESR spectra for low-spin Fe(III) porphyrins. At 77 K in CH_2Cl_2 containing tributylamine and 1-methylimidazole.

TABLE 1. ESR parameters for low-spin six-coordinate Fe(III) porphyrins[a]

Complex	g_1	g_2	g_3
N–Fe–N			
1c	2.88	2.27	1.54
2c	2.88	2.28	1.53
3c	2.89	2.28	1.52
O–Fe–N			
1c	2.57	2.17	1.82 (I)
	2.51		1.86 (II)
2c	2.55	2.18	1.83 (I)
	2.51		1.86 (II)
3c	2.63	2.18	1.83 (I)
	2.55		1.85 (II)
O–Fe–O			
3c	2.44		1.95

[a]At 77 K in CH_2Cl_2 containing tributylamine and 1-methylimidazole.

ratio of 1-methylimidazole to the porphyrins, and these spectra were assigned to the axial ligand systems, O–Fe–O, O–Fe–N and N–Fe–N. Their g values also fall within similar ranges to those observed for other Fe(III) porphyrins [6, 7, 11].

The ESR spectral signals of an O–Fe–O axial system are only observed for **3c** in the basic condition. One of the two oxygen atoms must originate from H_2O as an impurity in the solution, and another oxygen can be assigned to the phenolic OH (or O^-) on the picket fence of **3c**. Thus, at the low temperature of liquid N_2, the ligation of the phenolic group of this complex becomes feasible. This phenomenon may be closely

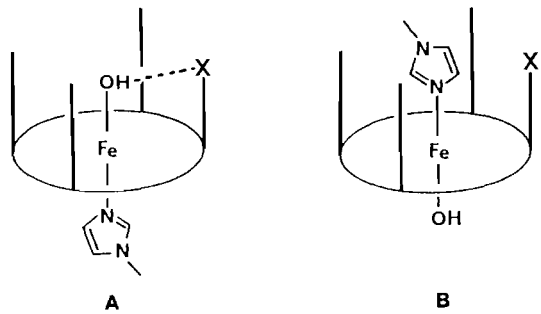

Fig. 4. Schematic representation of the two regioisomers of the picket fence porphyrin Fe(III) complexes with an O–Fe–N axial system.

related to the abnormal active sites of Hb M. However, it is not clear at present whether the ligation is intra- or intermolecular in character.

Another interesting feature of the ESR spectra is that two kinds of signals for the O–Fe–N axial system have been observed for all iron complexes. This can be attributed to the presence of two regioisomers as shown in Fig. 4. Some differences in the chemical properties of such regioisomers have also been reported for 'picnic-basket' porphyrin ruthenium complexes by Collman *et al.* [12]. In the present case, with an increase of the amount of 1-methylimidazole, Type II signals (Table 1) were preferentially converted to N–Fe–N type signals. Thus, it is likely that Type I signals are assignable to structure **A** which would be more stable than structure **B**.

Acknowledgement

This work was supported by a Grant-in-Aid for Scientific Research from the Ministry of Education (No. 01740351).

References

1 M. F. Perutz and H. Lehmann, *Nature (London), 219* (1968) 902.
2 P. D. Pulsinelli, M. F. Perutz and R. L. Nagel, *Proc. Natl. Acad. Sci. U.S.A., 70* (1973) 3870.
3 (a) N. Hayashi, Y. Motokawa and G. Kikuchi, *J. Biol. Chem., 241,* (1966) 79; (b) J. Greer, *J. Mol. Biol., 59* (1971) 107.
4 P. S. Gerald and M. L. Efron, *Proc. Natl. Acad. Sci. U.S.A., 47 (1961) 1758.*
5 E. W. Ainscough, A. W. Addison, D. Dolphin and B. R. James, *J. Am. Chem. Soc., 100* (1978) 7585.
6 C. Schaeffer, M. Momenteau, J. Mispelter, B. Loock, C. Huel and J.-M. Lhoste, *Inorg. Chem, 25* (1986) 4577.
7 (a) J. P. Collman, R. R. Gagne, C. A. Reed, T. R. Halbert, G. Lang and W. T. Robinson, *J. Am. Chem. Soc., 97* (1975)

1427; (b) J. P. Collman, J. I. Brauman, K. M. Doxsee, T. R. Halbert, S. E. Hayes and K. S. Suslick, *J. Am. Chem. Soc., 100* (1978) 2761.

8 J. P. Collman, J. I. Brauman, K. M. Doxsee, T. R. Halbert, E. Bunnenberg, R. E. Linder, G. N. LaMar, J. D. Gaudio, G. Lang and K. Spartalian, *J. Am. Chem. Soc., 102* (1980) 4182.

9 H. Imai and E. Kyuno, *Inorg. Chem., 29* (1990) 2416.

10 H. Imai, S. Sekizawa and E. Kyuno, *Inorg. Chim. Acta, 125* (1986) 151.

11 K. Tajima, J. Jinno, K. Ishizu, H. Sakurai and H. Ohya-Nishiguchi, *Inorg. Chem., 28* (1989) 709.

12 (a) J. P. Collman, J. I. Brauman, J. P. Fitzgerald, P. D. Hampton, Y. Naruta, J. W. Sparapany and J. A. Ibers, *J. Am. Chem. Soc., 110* (1988) 3477; (b) J. P. Collman, J. I. Brauman, J. P. Fitzgerald, J. W. Sparapany and J. A. Ibers, *J. Am. Chem. Soc., 110* (1988) 3486.